

Self-formation of sub-60-nm half-pitch gratings with large areas through fracturing

LEONARD F. PEASE III¹, PARU DESHPANDE², YING WANG², WILLIAM B. RUSSEL^{1*}
AND STEPHEN Y. CHOU^{2*}

¹Department of Chemical Engineering, Princeton University, Princeton, New Jersey 08544, USA

²Department of Electrical Engineering, Princeton University, Princeton, New Jersey 08544, USA

*e-mail: chou@princeton.edu; wbrussel@princeton.edu

Published online: 2 September 2007; doi:10.1038/nnano.2007.264

Periodic micro- and nanostructures (gratings) have many significant applications in electronic, optical, magnetic, chemical and biological devices and materials. Traditional methods for fabricating gratings by writing with electrons¹, ions² or a mechanical tip are limited to very small areas and suffer from extremely low throughput. Interference lithography can achieve relatively large fabrication areas, but has a low yield for small-period gratings^{3,4}. Photolithography⁵, nanoimprint lithography^{6,7}, soft lithography^{8,9} and lithographically induced self-construction¹⁰ all require a prefabricated mask, and although electrohydrodynamic instabilities¹¹ can self-produce periodic dots without a mask, gratings remain challenging. Here, we report a new low-cost maskless method to self-generate nano- and microgratings from an initially featureless polymer thin film sandwiched between two relatively rigid flat plates. By simply prising apart the plates, the film fractures into two complementary sets of nonsymmetrical gratings, one on each plate, of the same period. The grating period is always four times the thickness of the glassy film, regardless of its molecular weight and chemical composition. Periods from 120 nm to 200 μm have been demonstrated across areas as large as two square centimetres.

Low-cost and high-throughput patterning of nanogratings is essential to the fabrication and commercialization of a variety of nanodevices. The method described here, discovered in our studies of thin polymer films and termed fracture induced structuring (FIS), self-generates gratings on the nano- and microscale, with periods ranging from 120 nm to 200 μm . An initially featureless thin film is sandwiched between two relatively rigid flat plates that are then simply prised apart to produce two complementary gratings, without the need for masks, radiation, or sophisticated equipment or processing. Specifically, FIS consists of three steps (Fig. 1)^{12,13}. First, a coating of a polymer thin film (for example, spin casting of 15 kg mol^{-1} polystyrene that is 30–500 nm thick) is applied on a relatively rigid flat substrate (for example, a silicon wafer). Second, another plate is placed on top of the polymer film and the sandwich pressed while heating to ensure a good adhesion of the sandwiched film to the two plates. Third, the sandwich is separated (often by inserting a razor blade at one edge to prise the two plates apart). During the separation, the initially featureless polymer thin film breaks into two sets of gratings, the same in

period and complementary in shape, with one grating set on each plate.

Figure 2 shows the micrographs of typical top views and cross-sections of FIS gratings. The half-pitch of the FIS grating was found to be as small as 60 nm and as large as 120 μm . The cross-section of the FIS grating on each plate was found to be complementary but nonsymmetrical (that is, with different grating shape) (Fig. 2b–d). The 65-nm half-pitch grating came from a 31-nm-thick polystyrene film with a molecular weight (MW) of 1.3 kg mol^{-1} (Fig. 2e). The gratings with a half-pitch of 60 nm and smaller were also fabricated, but their spacing was not as regular as larger periods. To understand the mechanism of FIS, we investigated the effects of the thickness and mechanical properties of the polymer thin film, the adhesion between the polymer film and the plates, and process conditions in FIS. We discuss each of these in the following paragraphs.

One of our key observations is that the period p of the FIS grating depends solely on the film thickness h , scaled as $p = (4.0 \pm 0.6)h$. This relation holds over more than three orders of magnitude in film thicknesses, between 30 nm and 50 μm (hence a half-pitch from 60 nm to 100 μm), as shown in Fig. 3^{12,13}. The period does not depend on any other film properties or process conditions. Although the mechanical properties of the film do not affect the period, they do determine whether gratings may be observed. In particular, we found that FIS gratings will form as long as (a) the film consists of glassy material and not a rubbery or crystalline one, (b) the film remains below its glass transition temperature T_g and (c) the film exhibits good adhesion to both plates.

For example, we used a number of linear homopolymers: polystyrene, poly(methylmethacrylate) and polycarbonate of a broad range of MWs (for example, polystyrene of 2–1,400 kg mol^{-1} , which spans the entanglement MW of 13 kg mol^{-1}). All of them display FIS. Although polystyrene and poly(methylmethacrylate) are considered to be brittle, polycarbonate is known to be ductile, indicating the FIS process to be tolerant of moderate amounts of plasticity¹⁴. Similarly, other glassy materials do exhibit FIS gratings, including small-molecule glasses such as the disaccharides sucrose ($T_g \sim 70^\circ\text{C}$, $T_m \sim 170^\circ\text{C}$) and trehalose ($T_g = 106^\circ\text{C}$). On the other hand, FIS gratings did not form in rubbery or highly crosslinked polymer films (for example, UV-cured acrylates); rather, the separation between the thin film



Figure 1 Schematic of the FIS process. **a–c**, The process comprises the following steps. A thin glassy featureless film (yellow) is confined between two rigid plates (blue) (**a**), the two plates are prised apart from an edge, causing fracture of the film (**b**), and as the fracturing propagates from one edge of the plate to the other edge, the film self-breaks into two complementary sets of gratings of the same period but with nonsymmetrical shapes, one set on each plate (**c**).

and plate occurred along their flat interface, without disturbing the integrity of the polymer film. Furthermore, polycrystalline materials do not fracture into gratings, but leave behind a rough, aperiodic surface, presumably because local crystal anisotropy and heterogeneity prevent smooth propagation of the crack front.

Of similar import, we found good adhesion between the film and the plates to be essential to FIS grating formation (FIS will not form when adhesion is poor). By way of demonstration, we performed two tests. In the first, a monolayer of anti-adhesion molecules was coated at the interface between the film and a plate. We found the separation occurred simply along the flat interface and created no gratings in the polymer film. In the second test, we put the monolayer of anti-adhesion molecules only on parts of one plate, and found that after separation the FIS gratings formed only at the locations without the anti-adhesion layer (outside the rectangles on Fig. 2f), and not at the locations having the anti-adhesion layer, clearly demonstrating the important role of adhesion (and a method that selectively puts FIS gratings on a substrate). However, as already stated, we found that adhesion has

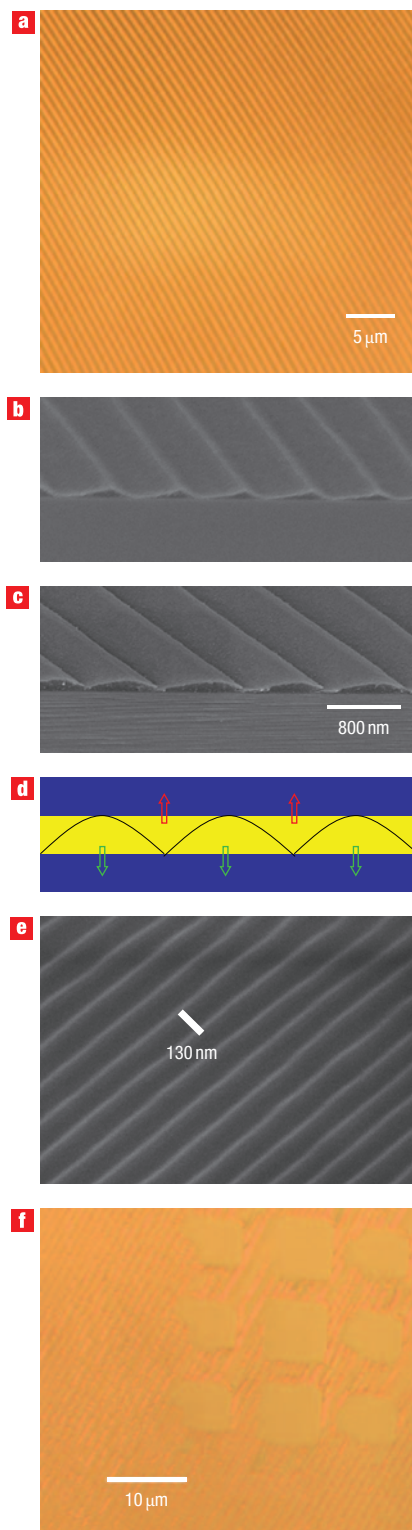


Figure 2 Images of FIS gratings. **a**, Optical micrograph of gratings of 800 nm pitch by FIS from a 200-nm-thick film of 15 kg mol^{-1} polystyrene. **b,c**, Cross-sectional SEM images of the gratings on each of the plates. **d**, Schematic of the relationship of the two complementary grating profiles. **e**, Half-pitch grating (65 nm), formed in a 31-nm-thick polystyrene film with MW 1.3 kg mol^{-1} . **f**, Optical micrograph of FIS gratings formed with one plate patterned with an anti-adhesion monolayer only inside the rectangles and otherwise good adhesion between the film and the plate, showing FIS gratings formed only in the areas with good adhesion.

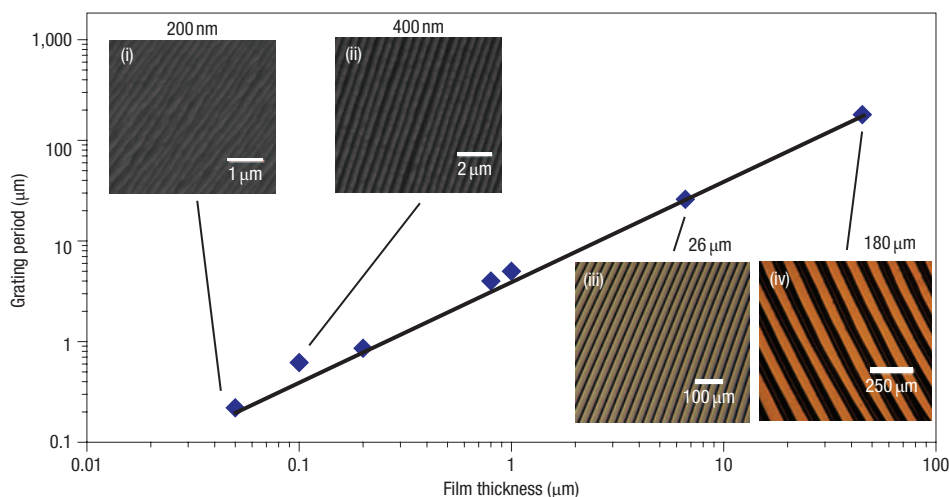


Figure 3 Grating period p as a function of film thickness h . Measurements were taken for films ranging in thickness from 30 nm to 50 μm . SEM micrographs in insets (i) and (ii) show gratings of 200 nm and 400 nm period, respectively, formed using 50-nm and 100-nm polystyrene films. The brighter lines indicate polymer raised from the surface. Optical micrographs (iii) and (iv) show gratings of 26 μm and 180 μm period, respectively, from a film thickness of 6.5 μm and 45 μm poly(methylmethacrylate) films, where lines of polymer are dark. For all data in this plot, separation was performed at room temperature.

Table 1 Effect of surface modification.

Bulk surface	2.1 kg mol ⁻¹ PS	47 kg mol ⁻¹ PS	Contact angle w/ H ₂ O
Bare silicon	Gratings	Gratings	20° ± 3°
Terminally anchored 2.7 kg mol ⁻¹ PS	Gratings	Gratings	60° ± 3°
Terminally anchored 57 kg mol ⁻¹ PS	Gratings	Gratings	72° ± 3°
Fluorinated surfactant (one side)	No gratings	No gratings	105° ± 3°

no effect on grating period. In fact, to further test the relationship between grating period and adhesion (note that the importance of this test is discussed with the mechanism below), we grafted different hydroxyl-terminated polystyrenes (PS) with MWs of 2.7 kg mol⁻¹ and 57 kg mol⁻¹ to silicon wafers through Si–O–C bonds (exceeding the strength of C–C bonds), but still found the grating period to be independent of the varying adhesion strength, eliminating a role for the energy of adhesion (Table 1).

Similarly, processing conditions affect whether the gratings will be observed. In particular, we found that FIS and the resulting grating period are not affected significantly by the temperature at which the plates are separated, as long as the temperature lies below T_g . If the separation temperature exceeds T_g , the FIS grating will not be formed. Figure 4 shows an experiment in polystyrene films (MW = 15 kg mol⁻¹) using different separation temperatures. When separation was performed above the polymer glass transition temperature ($\sim 105^\circ\text{C}$), no FIS grating formation was observed (for example, at 195 $^\circ\text{C}$, which is much higher than the T_g of $\sim 105^\circ\text{C}$). For separation temperatures from -200°C to 100 $^\circ\text{C}$ (just below T_g), the FIS gratings form and the period only increases slightly with temperature. This indicates that neither the annealing temperature nor viscous forces play a key role and confirms our previous finding that only glassy materials form gratings through fracture.

These results provide insight into possible underlying mechanisms. Of the several variables that could play a role in the

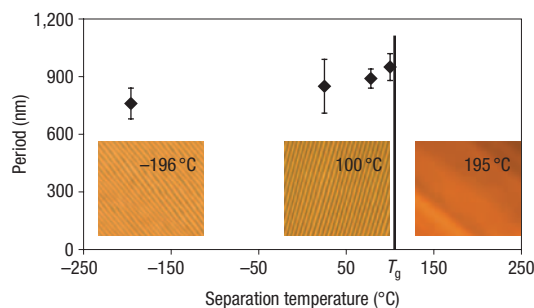


Figure 4 Grating period as a function of separation temperature. For a 200-nm-thick film of 15 kg mol⁻¹ polystyrene, when separation was performed above the polymer glass transition temperature T_g ($\sim 105^\circ\text{C}$), no FIS grating was observed. When the separation temperature changes from -196°C (boiling liquid nitrogen) to 100 $^\circ\text{C}$ (just below T_g), the FIS gratings form with period increasing slightly with temperature. The insets display typical results for separations at -196°C , 100 $^\circ\text{C}$ and 195 $^\circ\text{C}$, with dark lines indicating polymer raised from the surface. Error bars represent three standard deviations.

process, our experiments eliminate all but a few. Insensitivity to the strength of adhesion between the film and the plates (as demonstrated by the hydroxyl-terminated experiments) removes the energy of adhesion. Similarly, varying the MW from well below to well above the entanglement threshold eliminates a role for fracture toughness, as Kramer and co-workers¹⁵ note that “below the entanglement molecular weight (M_e) glassy polymers exhibit brittle behavior” and only above “2–3 M_e does the fracture energy increase rapidly and reach its maximum value”. Our observations resemble most closely those of Chai¹⁶, with brittle epoxy adhesives between aluminium plates in which the crack front remained orthogonal to the direction of propagation but oscillated from one substrate to the other, creating ridges parallel to the crack front with a period of approximately four times the layer thickness. They attributed the observed phenomena to cracks that became directionally unstable when

the radius of curvature of the semi-rigid plates being forced apart exceeds the thickness of the assembly.

Earlier analyses of trajectories by Cotterell and Rice¹⁷ indicate that stability of crack propagation depends on the ratio of stress normal to the bounding surfaces to that in the direction of propagation. When the latter becomes tensile, the crack should change direction to take advantage of the additional driving force. Subsequent analyses^{18,19} have refined the picture in terms of Mode I and Mode II cracking. The stress in the plane of the film depends critically on the geometry and the relative stiffnesses of the bounding plates, which affect the period. For example, more recent experiments²⁰ with one epoxy and one aluminium plate, an asymmetric geometry and a sol–gel adhesive produced similar fracture surfaces but with periods many orders of magnitude larger than the layer thickness. In both, the fracture seemed to remain cohesive, rather than adhesive²¹.

In summary, we report a new method for fabricating micro- and nanoscale gratings from glassy polymer films sandwiched between rigid plates. The method merely requires two flat, featureless substrates held together by a thin glassy film to be prised apart thereby transforming the initially featureless film into two complementary sets of gratings: one on one substrate and one on the other. We have examined several of the parameters governing the process and found the period to depend solely on the film thickness. Our experiments indicate brittle fracture to be responsible for the phenomena, which holds promise for applications in displays, nanophotonics and nanobiotechnology.

Received 4 June 2007; accepted 1 August 2007; published 2 September 2007.

References

- Tennant, D. M. *et al.* Characterization of near-field holography grating masks for optoelectronics fabricated by electron-beam lithography. *J. Vac. Sci. Technol.* **10**, 2530–2535 (1992).
- Melngailis, J., Mondelli, A. A., Berry, I. L. & Mohondro, R. A review of ion projection lithography. *J. Vac. Sci. Technol.* **16**, 927–957 (1998).
- Yen, A., Anderson, E. H., Ghanbari, R. A., Schattenburg, M. L. & Smith, H. I. Achromatic holographic configuration for 100 nm-period lithography. *Appl. Opt.* **31**, 4540–4545 (1992).
- Solak, H. H. *et al.* Exposure of 38 nm period grating patterns with extreme ultraviolet interferometric lithography. *Appl. Phys. Lett.* **75**, 2328–2330 (1999).
- Hill, K. O., Malo, B., Bilodeau, E., Johnson, D. C. & Albert, J. Bragg gratings fabricated in monomode photosensitive optical fiber by UV exposure through a phase mask. *Appl. Phys. Lett.* **62**, 1035–1037 (1993).
- Chou, S. Y., Krauss, P. R. & Renstrom, P. J. Imprint lithography with 25-nanometer resolution. *Science* **272**, 85–87 (1996).
- Bailey, T. *et al.* Step and flash imprint lithography: Template surface treatment and defect analysis. *J. Vac. Sci. Technol.* **18**, 3572–3577 (2000).
- Kumar, A. & Whitesides, G. M. Features of gold having micrometer to centimeter dimensions can be formed through a combination of stamping with an elastomeric stamp and an alkanethiol ink followed by chemical etching. *Appl. Phys. Lett.* **63**, 2002–2004 (1993).
- Duffy, D. C., McDonald, J. C., Schueller, O. J. A. & Whitesides, G. M. Rapid prototyping of microfluidic systems in poly(dimethylsiloxane). *Anal. Chem.* **70**, 4974–4984 (1998).
- Chou, S. Y., Zhuang, L. & Guo, L. J. Lithographically induced self-construction of polymer microstructures for resistless patterning. *Appl. Phys. Lett.* **75**, 1004–1006 (1999).
- Chou, S. Y. & Zhuang, L. Lithographically induced self-assembly of periodic polymer micropillar arrays. *J. Vac. Sci. Technol.* **17**, 3197–3202 (1999).
- Deshpande, P. Nanolithography in thin polymer films using guided self-assembly. PhD Dissertation, Princeton University (2005).
- Pease, L. F. III. Pattern formation in polymer via electrohydrodynamic instabilities and glassy fracture. PhD Dissertation, Princeton University (2005).
- Bjerke, T., Li, Z. H. & Lambros, J. Role of plasticity in heat generation during high rate deformation and fracture of polycarbonate. *Int. J. Plasticity* **18**, 549–567 (2002).
- Benkoski, J. J., Fredrickson, G. H. & Kramer, E. J. Model for the fracture energy of glassy polymer–polymer interfaces. *J. Polym. Sci.* **40**, 2377–2386 (2002).
- Chai, H. A note on crack trajectory in an elastic strip bounded by rigid substrates. *Int. J. Fracture* **32**, 211–213 (1987).
- Cotterell, B. & Rice, J. B. Slightly curved or kinked cracks. *Int. J. Fracture* **16**, 155–169 (1980).
- Sumi, Y., Nemat-Nasser, S. & Keer, L. M. On crack path stability in a finite body. *Eng. Fracture Mech.* **22**, 759–771 (1985).
- Wang, J. S. & Suo, Z. Experimental determination of interfacial toughness curves using brazil-nut sandwiches. *Acta Metall. Mater.* **38**, 1279–1290 (1990).
- Liu, J. *et al.* Fracture behavior of an epoxy/aluminum interface reinforced by sol–gel coatings. *J. Adhesion Sci. Technol.* **20**, 277–305 (2006).
- Freund, L. B. *Dynamic Fracture Mechanics* (Cambridge Univ. Press, Cambridge, 1998).

Acknowledgements

This work was supported by the Materials Research Science & Engineering Centers (MRSEC) (NSF-DMR-0213706), the Defence Advanced Research Projects Agency (DARPA), the Office of Naval Research (ONR) and the Department of Defense (NDSEG) through a fellowship to L.E.P. The authors thank Wen-di Li for preparation of certain graphs. Correspondence and requests for materials should be addressed to S.Y.C.

Author contributions

P.D., L.E.P. and Y.W. performed the experiments. L.F.P., P.D., Y.W., W.B.R. and S.Y.C. designed and discussed the experiments, analysed the data and co-wrote the paper.

Competing financial interests

The authors declare no competing financial interests.

Reprints and permission information is available online at <http://npg.nature.com/reprintsandpermissions/>